Efficient Evaluation of Spatial-Domain MoM Matrix Entries in the Analysis of Planar Stratified Geometries

Noyan Kinayman and M. I. Aksun

Abstract—An efficient hybrid method for evaluation of spatial-domain method-of-moments (MoM) matrix entries is presented in this paper. It has already been demonstrated that the introduction of the closed-form Green's functions into the MoM formulation results in a significant computational improvement in filling up MoM matrices and, consequently, in the analysis of planar geometries. To achieve further improvement in the computational efficiency of the MoM matrix entries, a hybrid method is proposed in this paper and, through some examples, it is demonstrated that it provides significant acceleration in filling up MoM matrices while preserving the accuracy of the results.

Index Terms—Closed-form spatial-domain Green's functions, method of moments, printed circuits.

I. INTRODUCTION

The method of moments (MoM) is one of the widely used numerical techniques employed for the solution of mixed potential integral equations (MPIE's) [1]–[3] arising in the analysis of planar stratified geometries. Recently, the computational burden of the spatial-domain MoM, which is evaluations of the Sommerfeld integrals, has been alleviated by introducing an efficient algorithm to approximate these integrals in closed-form expressions, resulting in closed-form spatial-domain Green's functions [4], [5]. Consequently, the central processing unit (CPU) time required to calculate the MoM matrix entries, also known as "fill-time," has been reduced considerably. Following this development, it was also shown that the reaction integrals (MoM matrix entries) resulting from the application of the MoM in conjunction with the closed-form Green's functions can also be evaluated analytically, which further improves the computational efficiency of the spatial-domain MoM [6].

In this paper, a new hybrid method based on the use of the technique outlines in [6], in the vicinity of the source and a simpler approximation algorithm, elsewhere, is developed and presented. It is also demonstrated that this hybrid method has significantly accelerated the matrix fill-in time as compared to the original approach presented in [6]. The application of the hybrid method is provided for a realistic example, and possible difficulties together with their remedies are discussed.

II. THE HYBRID METHOD

Evaluation of MoM matrix entries is the one that requires most of the CPU time of the technique for moderate-size geometries (spanning a few wavelengths). To give an idea, CPU times for the evaluations of the Green's functions, matrix entries, and the solution of the MoM matrix equation are given in Table I for some typical printed geometries. Note that the geometries referred to in Table I have been analyzed

with uniform segmentation, which gives rise to block symmetric MoM impedance matrices. Detailed study of hybrid method for the interdigital capacitor mentioned in Table I will be provided in the following sections. Due to space limitations, results for the patch antenna and the bandpass filter could not be provided.

In order to introduce the hybrid method, let us first write down the spatial-domain MoM matrix entry of a planarly stratified geometry obtained through the MPIE formulation [1], [2]

$$Z_{mn} = \langle T_{xm}, G_{xx}^A * J_{xn} \rangle + \frac{1}{w^2} \left\langle T_{xm}, \frac{\partial}{\partial x} \left[G_x^q * \frac{\partial J_{xn}}{\partial x} \right] \right\rangle \tag{1}$$

where T_{xm} are the testing functions, J_{xn} are the basis functions, and $\langle \, , \, \rangle$ is the inner product. The spatial-domain Green's functions employed in (1) are obtained in closed forms with the use of the two-level approach described in [7], which have the generic form of

$$G^{A, q} \cong \sum_{n=1}^{N} a_n \frac{e^{-jk_i r_n}}{r_n} \tag{2}$$

where $r_n = \sqrt{\rho^2 - b_n^2}$, $\rho = \sqrt{x^2 + y^2}$, k_i is the wavenumber in source layer, and b_n is the complex constant. It has been demonstrated in [6] that the MoM matrix entries given in (1) can be calculated analytically without any numerical integration for piecewise-continuous basis and testing functions, provided the closed-form Green's functions are used for the formulation. In that approach, each of the exponentials in (2) is replaced by its Taylor series approximation as follows:

$$G^{A, q} \cong \sum_{n=1}^{N} a_n \sum_{m=0}^{M} c_{mn} \frac{(r_n - r_c)^m}{r_n} \tag{3}$$

where c_{mn} are the Taylor series coefficients and r_c is the center of expansion for the exponential term $e^{-jk_i r_n}$. Alternatively, one could replace the entire Green's function in (2) with a suitable approximation that would enable the reaction integrals to be evaluated analytically. For instance, one may use the polynomial approximation for the Green's function as

$$G^{A, q} \cong \sum_{l=-1}^{L} \gamma_l \cdot \rho^l \tag{4}$$

where γ_l are complex coefficients obtained from a least-squares (LS) fitting scheme. It is obvious that the analytical integration of the reaction integrals is considerably simpler for the Green's function expressed in (4) than for those expressed in (3). This is because the analytical evaluation of the inner-product integrals using the former representation requires extensive complex arithmetic operations, as well as multiple evaluations of complex logarithms and trigonometric functions. However, the caveat in the polynomial-fitting approach is that the approximating the Green's function over the entire range is very difficult, if not impossible, with a relatively small L, because of the singular behavior of the Green's functions as $\rho \to 0$. One approach to resolving this dilemma is to utilize both of the above representations, but in complementary regions, thereby taking the advantage of the salient features of both. This can be done by using (3) to represent the Green's function for small ρ, where it exhibits a singular behavior, and then by switching over to (4) as ρ becomes larger.

To summarize, a direct application of the rigorous method places an unnecessary computational burden when ρ, the distance between the source and testing points, is greater than a predetermined value $\rho_{ls} = 10^s/k_0$, where s is a constant. To circumvent this problem, one can use a hybrid approach as given in (5), which uses a judicious combination

TABLE I
CPU TIMES IN SECONDS REQUIRED FOR THE ANALYSIS OF SOME TYPICAL GEOMETRIES AT SINGLE FREQUENCY ON A SUN SPARC ULTRA-2 WORKSTATION. HYBRID METHOD INCLUDES THE ADAPTIVE SELECTION OF ρ_{ls}, AS EXPLAINED IN SECTION II

Geometry	# of unknowns	Analysis frequency (MHz)	Green's function computation time (sec.)	Matrix fill-time (sec.)		Solution time (sec.)
				Hybrid	Rigorous	
Patch antenna [8]	537	2300	2.3	7	63	30
Band-pass filter [9]	1638	2575	2.3	23	570	1100
Interdigital MIC capacitor (Fig. 1)	576	5500	2.3	9	187	39

of the two methods, to increase the computational speed with which the MoM matrix entries are generated as follows:

$$Z_{mn}^{q,A} = \begin{cases} \int\int f(u)g(v) \sum_{n=1}^{N} a_n \dfrac{e^{-jk_i\sqrt{u^2+v^2-b_n^2}}}{\sqrt{u^2+v^2-b_n^2}}\, du\, dv, \\ \qquad\qquad\qquad\qquad\qquad \rho < \rho_{ls} \quad (5a) \\ \int\int f(u)g(v) \sum_{l=-1}^{L} \gamma_l \rho^l\, du\, dv, \qquad \rho \geq \rho_{ls}. \quad (5b) \end{cases}$$

For rooftop basis and testing functions, $f(u)$ and $g(v)$ are given as

$$f(u) = \alpha_0 + \alpha_1 u + \alpha_2 u^2 + \alpha_3 u^3 \qquad (6)$$
$$g(v) = \beta_0 + \beta_1 v \qquad (7)$$

where α and β are constants obtained from the correlation operation of the basis and testing functions [6].

At this point, it is worthwhile to describe the strategy for employing the hybrid technique. To use a small L in (4) and simplify the algorithm, the polynomial-fitting algorithm is performed over a small range of ρ, which is requires the LS fitting with N_{ls} sampling points to be repeated for each of the inner-product operations. Consequently, to accelerate the fitting process, the closed-form Green's function is sampled between ρ_{ls} and $\rho_{\max}$, and the sampled values are stored in a look-up table before starting to fill up the MoM matrix. These tabulated values can then be subsequently interpolated to perform the LS fitting relatively fast for each inner product operation. Here, one can use linear or quadratic interpolation scheme to find required values for the LS approximation process from the previously sampled values of the Green's function whose effects will also be demonstrated.

For a given geometry, either user can specify the value of ρ_{ls} through s or it can be determined adaptively by using the rms fitting error in the LS approximation scheme. The adaptive approach, which is the one used throughout this paper, starts with an error criterion defined as in following form:

$$\sqrt{\frac{1}{N_e}\sum_{i=0}^{N_e}\left[G_{\text{method} \#1}^{A,q} - G_{\text{method} \#2}^{A,q}\right]^2} \leq E \qquad (8)$$

where $G_{\text{method} \#1}^{A,q}$ corresponds to the Green's function approximations obtained from (3), $G_{\text{method} \#2}^{A,q}$ corresponds to the Green's function approximations obtained from (4), E is the acceptable rms fitting error, and N_e is the number of samples used in error checking ($N_e > N_{ls}$). Then, since the LS approximation in (4) is implemented over a range of $\rho(\rho_a \leq \rho \leq \rho_b)$, the lower and upper limits ρ_a and ρ_b, respectively, are determined adaptively starting with the initial values of minimum cell width and maximum possible ρ value for the inner product evaluation, respectively. If the condition specified by (8) is satisfied, ρ_{ls} is set to
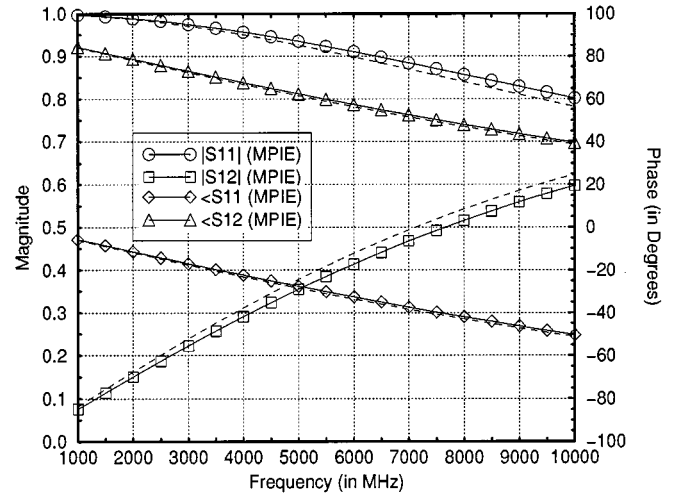
Fig. 1. S_{11} and S_{12} of the interdigital capacitor given in Fig. 2. The dashed lines represent the results from *em* by Sonnet Software, Inc, Liverpool, NY.

ρ_a and the iteration is terminated, otherwise ρ_a is increased by a small increment $\Delta\rho$, and the iteration continues until (8) is satisfied. This approach makes the hybrid method a very suitable tool for designing an efficient MoM-based electromagnetic simulator. In the examples given in Table I, the constant E was selected as 10^{-5}.

III. NUMERICAL EXAMPLES

To study the effectiveness and accuracy of the hybrid method proposed in this paper, CPU times for different parameter setting and scattering parameters (S-parameters) of an example printed structure are obtained using the rigorous and hybrid methods. The example selected here is an interdigital microwave integrated circuit (MIC) capacitor whose S-parameters and geometry are shown in Figs. 1 and 2, respectively. Number of basis functions for the interdigital capacitor is chosen to be 576. For the sake of fairness, an error term is defined as

$$\text{error} = \sqrt{\sum_{i=1}^{N_p} \left| S_{1i}^{\text{rigorous}} - S_{1i}^{\text{hybrid}} \right|^2} \qquad (9)$$

where N_p is the number of ports in the structure. The matrix fill time for this geometry could be reduced by changing the auxiliary parameter s, as shown in Fig. 2 ($L = 4$, $N_{ls} = 9$). Note that the matrix fill time for each s value given in the figure is the accumulative fill time over frequency in the simulation band, whereas the times given in Table I are at single frequency. To find the average fill time at a single frequency, the
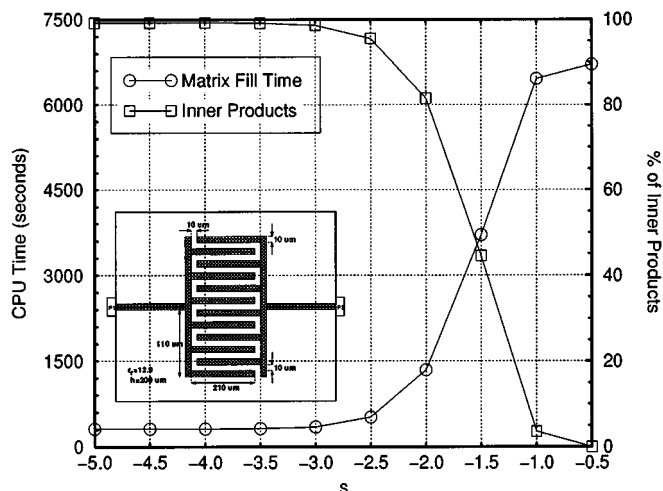
Fig. 2. Total matrix and percentage of inner-products that fall in the LS approximation region for the interdigital capacitor (1000 MHz $\leq f \leq 10\,000$ MHz, $\Delta f = 250$ MHz).

Fig. 4. Error in S_{11} and S_{12} of the interdigital capacitor for different values of s [error is defined in (9)].
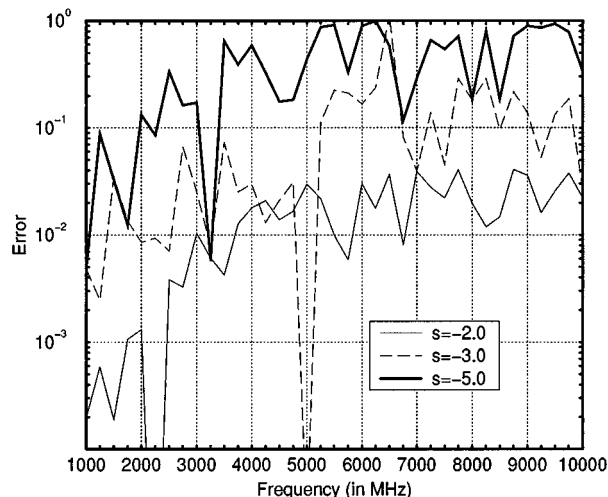
Fig. 3. Error in S_{11} and S_{12} of the interdigital capacitor for different values of s [error is defined in (9)].

time values read from Fig. 2 should be divided by the number of simulation points, which in this case is 37. From the figure, it is observed that the matrix fill time is saturated around $s = -3.0$, providing a considerable amount of reduction in the matrix fill time. However, the error in S-parameters is relatively high at some frequency points, and the situation is even worse at $s = -5.0$, as shown in Fig. 3. This could be attributed to a poor approximation of the Green's functions by the polynomials given in (4). It is also observed that the error in S-parameters increases even though the percentage of the inner products evaluated through the LS fitting scheme does not increase. This is due to fact that, although the value of ρ_{ls} below some point cannot change the matrix fill time (unless it becomes zero), the algorithm keeps sampling the Green's functions starting from lower and lower ρ values as ρ_{ls} is decreasing. However, such choices of ρ_{ls} only occur in cases of manually varying the value of s; in practice, there is a minimum limit (usually the minimum cell width) on the value of ρ_{ls} and it is determined by the adaptive algorithm that was previously described.

As a next step, the number of sampling points, i.e., N_{ls}, is increased from 9 to 12, and the error in S-parameters is calculated again for $s = -5.0$, giving the results in Fig. 4. While there is a noticeable im-

provement in the average error, the error is still not acceptable at higher frequency points. Thus far, we have only employed linear interpolation with nine interpolation points, for which the results given in Fig. 3 have higher error for $s = -5.0$. Although increasing the interpolation points from 9 to 12 in the linear LS approximation has improved the results to a degree, they are still not acceptable (Fig. 4). However, switching to quadratic interpolation from linear interpolation gives a significant improvement even for the smaller values of s, as shown in Fig. 4.
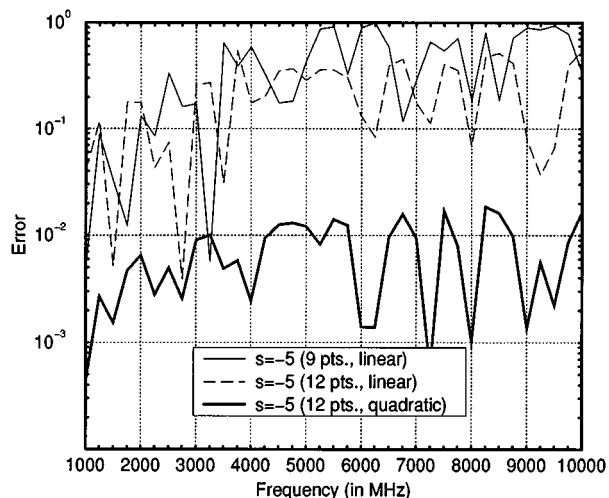
IV. CONCLUSIONS

In this paper, it has been demonstrated that the hybrid method significantly improves the efficiency of the evaluation of spatial-domain MoM matrix entries, on the order of tenfold to twentyfold reduction in matrix fill time. Therefore, even for moderate-size geometries, the solution time of the matrix equations becomes the dominating factor on the overall performance of the spatial-domain MoM. Consequently, the spatial-domain MoM in conjunction with the closed-form Green's functions has become a powerful computer-aided design (CAD) tool for the analysis of planar structures, provided that the hybrid method presented in this paper is employed in the evaluation of the matrix entries.

REFERENCES

[1] J. R. Mosig and F. E. Gardiol, "General integral equation formulation for microstrip antennas and scatterers," *Proc. Inst. Elect. Eng.*, pt. H, vol. 132, pp. 424–432, Dec. 1985.
[2] J. R. Mosig, "Arbitrarily shaped microstrip structures and their analysis with a mixed potential integral equation," *IEEE Trans. Microwave Theory Tech.*, vol. 36, pp. 314–323, Feb. 1988.
[3] W. C. Chew, *Waves and Fields in Inhomogeneous Media*. New York: Van Nostrand, 1990.
[4] Y. L. Chow, J. J. Yang, D. G. Fang, and G. E. Howard, "A closed-form spatial Green's function for the thick microstrip substrate," *IEEE Trans. Microwave Theory Tech.*, vol. 39, pp. 588–592, Mar. 1991.
[5] M. I. Aksun and R. Mittra, "Derivation of closed-form Green's functions for a general microstrip geometry," *IEEE Trans. Microwave Theory Tech.*, vol. 40, pp. 2055–2062, Nov. 1992.
[6] L. Alatan, M. I. Aksun, K. Mahadevan, and T. Birand, "Analytical evaluation of MoM matrix elements," *IEEE Trans. Microwave Theory Tech.*, vol. 44, pp. 519–525, Apr. 1996.
[7] M. I. Aksun, "A robust approach for the derivation of closed-form Green's functions," *IEEE Trans. Microwave Theory Tech.*, vol. 44, pp. 651–658, May 1996.
[8] D. M. Pozar, "Input impedance and mutual coupling of rectangular microstrip antennas," *IEEE Trans. Antennas Propagat.*, vol. AP-30, pp. 1191–1196, Nov. 1982.

[9] J.-S. Hong and M. J. Lancaster, "Couplings of microstrip square open-loop resonators for cross-coupled planar microwave filter," *IEEE Trans. Microwave Theory Tech.*, vol. 44, pp. 2099–2109, Dec. 1996.

CAD Models for Asymmetrical, Elliptical, Cylindrical, and Elliptical Cone Coplanar Strip Lines

Zhengwei Du, Ke Gong, Jeffrey S. Fu, Zhenghe Feng, and Baoxin Gao

Abstract—By the conformal mapping method, we give analytical closed form expressions for the quasi-TEM parameters for asymmetrical coplanar strip lines (ACPS's) with finite boundary substrate. Then, based on the analysis of ACPS's, elliptical coplanar strip lines (ECPS's) and cylindrical coplanar strip lines (CCPS's), and elliptical cone coplanar strip lines (ECCPS's) are studied. Computer-aided-design oriented analytical closed-form expressions for the quasi-TEM parameters for ACPS's, ECPS's, CCPS's, and ECCPS's are obtained. All of the expressions are simple and accurate for microwave circuits' designs and are useful for transmission-line theory and antenna theory. The reasonableness of the method and results are verified and various design curves are given.

Index Terms—Asymmetrical coplanar strip lines, CAD modes, conformal mapping, cylindrical coplanar strip lines, elliptical cone coplanar strip lines, elliptical coplanar strip lines.

I. INTRODUCTION

Coplanar transmission lines are used extensively in monolithic microwave integrated circuits (MMIC's) and integrated optical applications [1], [2]. An asymmetrical coplanar transmission line consists of a narrow metal strip and a conductive plane grounded, which are placed on one side of the dielectric substrate and mutually separated by a narrow slot. The advantage is the possibility of combination with other types of transmission lines such as a slot line, coplanar waveguide, and microstrip when used in filters, impedance matching networks, and directional couplers. In the earlier years, coplanar strip lines (CPS's) were analyzed by assuming that the substrate is infinite [3], [4]. In recent years, people obtained the expressions for the quasi-TEM parameters for CPS's on a substrate [5], [6] and multilayer substrates [7]–[10] of finite thickness. The problem of a CPS with a substrate of finite thickness and finite width has not been solved up to now.

Elliptical coplanar strip lines (ECPS's), cylindrical coplanar strip lines (CCPS's), and elliptical cone coplanar strip lines (ECCPS's) can be used as adapters and slot lines as well as antennas. Although elliptical [11] and elliptical cone [12], [13] striplines and microstrip lines have been analyzed, the analyzes of ECPS's and ECCPS's have not been reported to our knowledge. In [14] and [15] closed form expressions for quasi-TEM parameters for CCPS's were given. Both [14] and [15] treated the width of the substrate as infinite when the CCPS was mapped into the ACPS, while the width should be 2π. In addition, there is an error in [15] as pointed out in this paper.

The objective of this paper is to solve the problems mentioned above. Assuming that the ACPS with a finite-boundary dielectric substrate of finite thickness and width, ECPS, CCPS, and ECCPS are operating in the quasi-TEM mode, the conformal mapping method is used for the analysis. The assumption is valid when the length of a line is much longer than the wavelength of the guided wave and the operating frequency of the guided wave is not high. This method can give fast and accurate results in the microwave frequency range since the quasi-TEM parameters for coplanar lines are only slightly sensitive to changes in the frequency [15]. As the substratum, we study the quasi-TEM parameters for the ACPS with finite boundary substrates at first. In Sections III and IV, ECPS's, CCPS's, and ECCPS's are analyzed. In Section V, the reasonableness of the method and results are verified, and numerical results for the characteristic impedance for the ACPS with finite boundary substrate, ECPS, CCPS, and ECCPS are given.

II. ACPS WITH FINITE BOUNDARY SUBSTRATE

The analyzed ACPS on a finite-boundary substrate is shown in Fig. 1(a). The widths of the infinitely long strips are w_1 and w_2 and the gap between them is $2s$. The two strips are mounted on a substrate having a thickness of h, a width of $2w$, and a relative dielectric constant of ε_r. In this case, the ACPS capacitance C is $C = C_0 + C_1$, where C_0 is the ACPS capacitance in free space when the dielectric is replaced by air, and C_1 is the ACPS capacitance obtained when assuming that the electric field is concentrated in a dielectric of thickness h, width $2w$, and relative dielectric constant of $\varepsilon_r - 1$. This assumption has shown an excellent accuracy in the cases of the CPS and ACPS with a finite thickness and infinite width substrate [5]–[8].

The free-space capacitance C_0 is given by [9]

$$C_0 = \varepsilon_0 \frac{K(k_0')}{K(k_0)} \tag{1}$$

where k_0 is shown in (2) at the bottom of the following page. In order to obtain the capacitance C_1, the dielectric region in Fig. 1(a) is mapped into the lower half region, as shown in Fig. 1(b), by the Jacobian elliptic function transformation $t = sn((K(k)/w)z, k)$, where $K(k)$ is the complete elliptic integral of the first kind of modulus k, $K(k)/K(k') = w/h$, and $k' = \sqrt{1 - k^2}$. For simplified calculation, the excellent approximate expressions of k are given by [16]

$$k = \left[\frac{\exp(\pi w/h) - 2}{\exp(\pi w/h) + 2}\right]^2, \qquad \text{for } 1 \leq \frac{w}{h} < \infty \tag{3a}$$

$$k = \sqrt{1 - \left[\frac{\exp(\pi h/w) - 2}{\exp(\pi h/w) + 2}\right]^4}, \qquad \text{for } 0 < \frac{w}{h} < 1. \tag{3b}$$

The widths s, w_1, and w_2 are mapped s_t, w_{1t}, and w_{2t}, which can be expressed as follows:

$$s_t = t_1 = sn\left(\frac{K(k)}{w}s, k\right) \tag{4a}$$

$$w_{1t} = t_2 - t_1 = sn\left(\frac{K(k)}{w}(s + w_1), k\right) - sn\left(\frac{K(k)}{w}s, k\right) \tag{4b}$$

$$w_{2t} = t_3 - t_1 = sn\left(\frac{K(k)}{w}(s + w_2), k\right) - sn\left(\frac{K(k)}{w}s, k\right). \tag{4c}$$